Supporting Information

Osz et al. 10.1073/pnas.1118192109

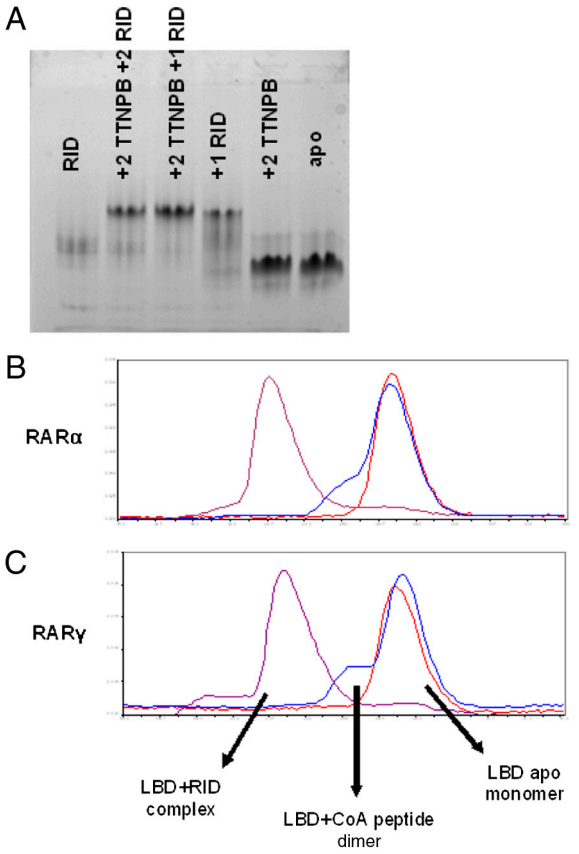

Fig. S1. Coactivator bound-RARβ LBD forms homodimers in solution. (*A*) Native PAGE of SRC-1 RID alone (lane 1), RARβ LBD with two equivalents of TTNBP and two equivalents of SRC-1 RID (lane 2), RARβ LBD with two equivalents of TTNPB and one equivalent of SRC-1 RID (lane 3), RARβ LBD with one equivalent of SRC-1 RID (lane 4), RARβ LBD with two equivalents of TTNPB (lane 5) and RARβ LBD apo (lane 6). (*B*) Gel filtration profiles of apo RARα and the TTNPB complexes with SRC-1 NR2 or SRC-1 RID. (*C*) Gel filtration profiles of apo RARγ and the TTNPB complexes with SRC-1 NR2 or SRC-1 RID.

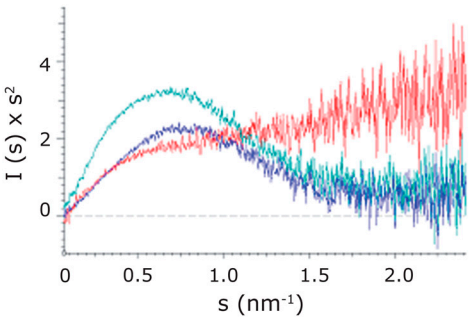

Fig. S2. Kratky plot from small angle X-ray scattering results showing the folding of SRC-1 RID upon binding to RARβ LBD. SRC-1 RID in red, RARb LBD-SRC-1 NR2 in blue, and RARb LBD-SRC-1 RID complex in cyan.

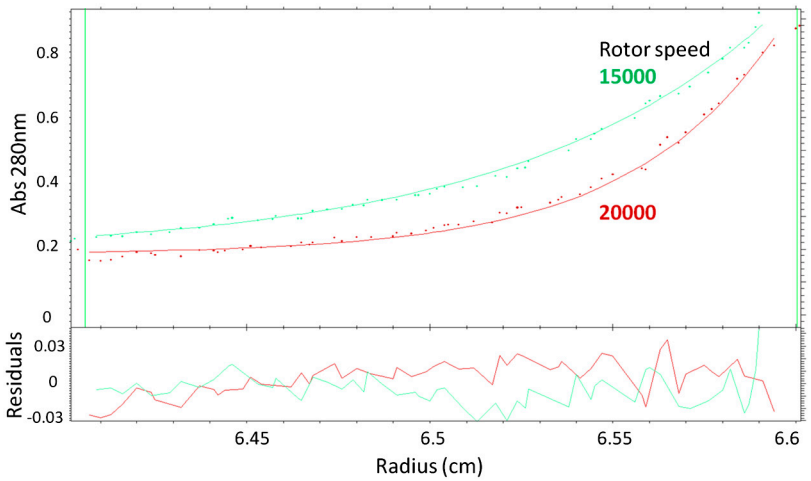

Fig. S3. Sedimentation equilibrium experiments. Best fits of experimental data for RARβ LBD-TTNPB-SRC-1 RID (4 °C) at 15,000 and 20,000 rpm with the self-association methods (SedPhat program—*Methods*). The random distribution of the residuals (*Bottom*) indicates that the fit is satisfactory. Sedimentation equilibrium data of RARβ LBD-TTNPB-SRC-1 RID agree with one SRC-1 RID bound to a homodimer of RARβ LBD. (see *Results* and *Discussion* for details).

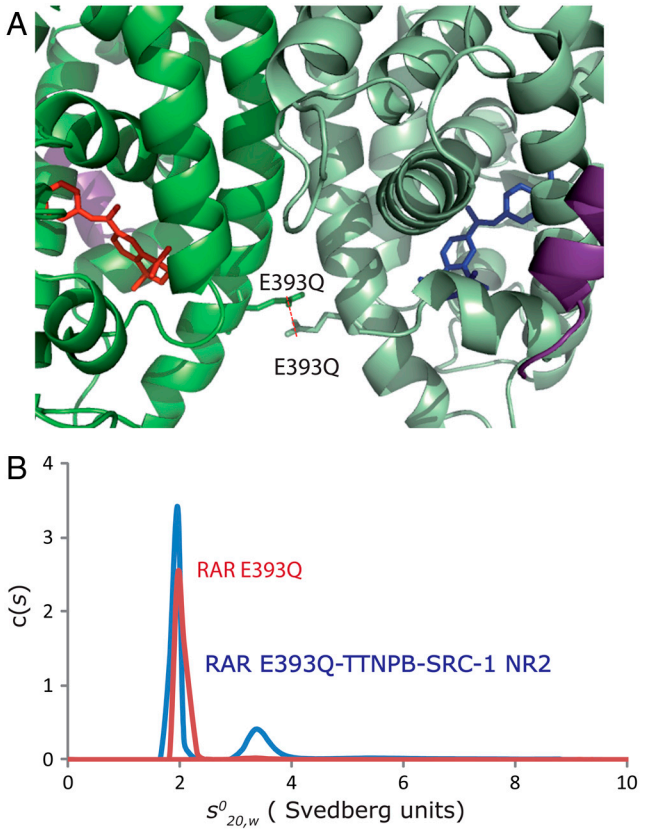

Fig. S4. Characterization of RAR E393Q LBD, a residue shown to be important in the dimer communication. (*A*) Model of RARα E393Q dimer with Q393 of one monomer interacting with Q393 of the other monomer. (*B*) Sedimentation velocity analysis for RARα E393Q LBD apo and its complexes with TTNPB and SRC-1 NR2 peptide by Lamm equation fits using the Sedfit program. The sedimentation distribution plot shows one sedimentation species for the apo RARα E393Q LBD. In presence of ligand and SRC-1 NR2 peptide, two peaks are observed, one corresponding to the monomer and the second to the dimer.

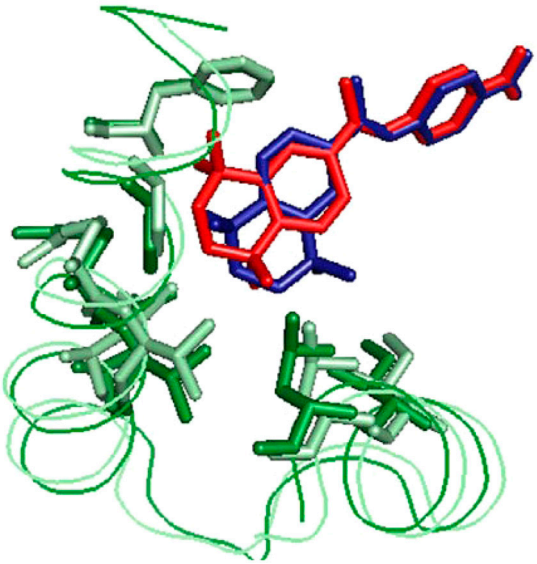

Fig. S5. Different conformations of TTNPB ligands in each monomer. Close-up view of the interactions of TTNPB near the tetrahydronaphthalene region, in the ligand binding pockets of M1 (green) and M2 (light green) of the RARβ LBD homodimer.

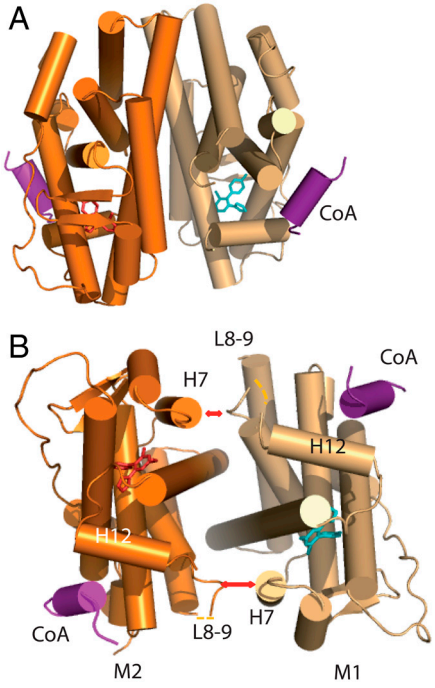

Fig. S6. Crystal structure of ERβ LBD-RU100132-SRC-1 NR2. (*A*) Overall structure of ERα homodimer. (*B*) View along the pseudo-twofold axis of the homodimer LBD of hERα. Red arrows highlight the dissymmetrical distances between ERα's helix H7 and loop L8-9.

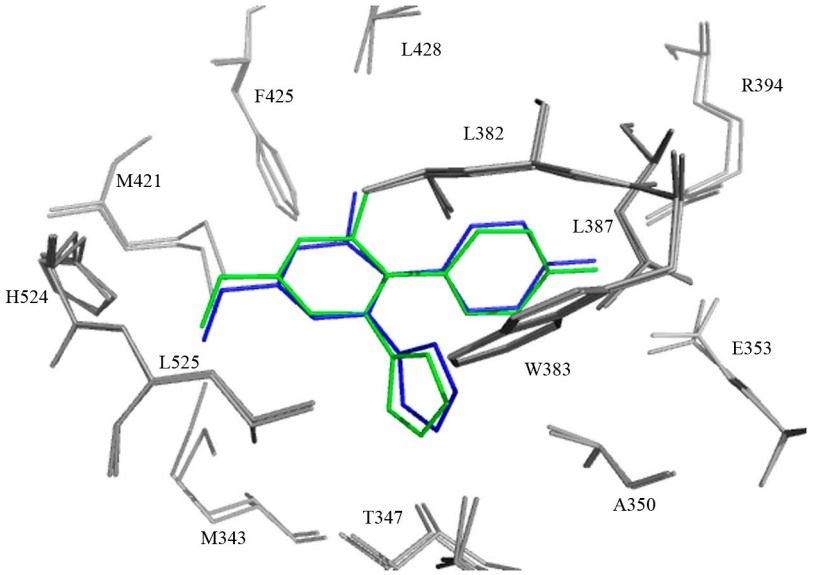

Fig. S7. Interactions made by RU100132 ligand in each monomer of the homodimeric hERα LBD. Some differences in the position of the ligands and in their contacts are observed between the two monomers, as for example Arg394 (H5) and its contacts with RU100132 (2.9 Å in one monomer and 3.3 Å in the other).

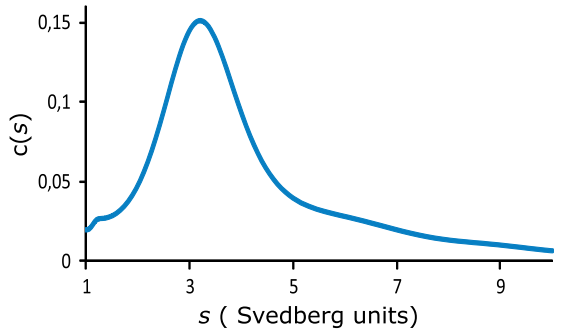

Fig. S8. SRC-1 RID coactivator binds ERβ LBD with a stoichiometry of one coactivator per dimer. Sedimentation velocity analysis for ERβ LBD in complex with estradiol and SRC-1 RID. The sedimentation distribution plots show one sedimentation specie with the corresponding sedimentation coefficient 3.34S that corresponds to a molecular mass value of 84,500 Da.

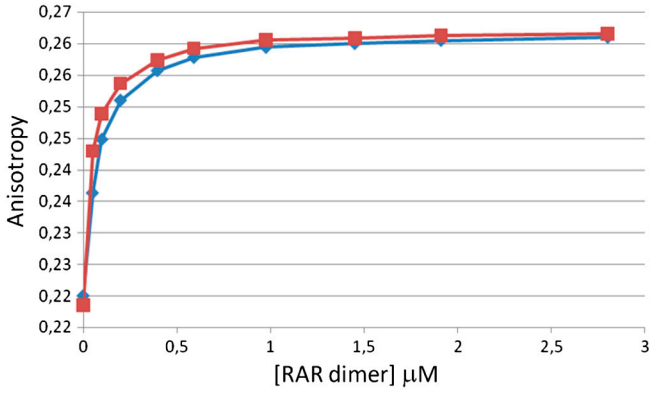

Fig. S9. Binding curve of RARαΔAB-RARαΔAB in absence (blue squares) and presence of SRC-1 NR2 peptide (red squares) to the FAM-labeled DR2 DNA. The binding constants to the oligonucleotides were determined from anisotropy titrations with FAM-labeled DR2, as described in *Methods*.

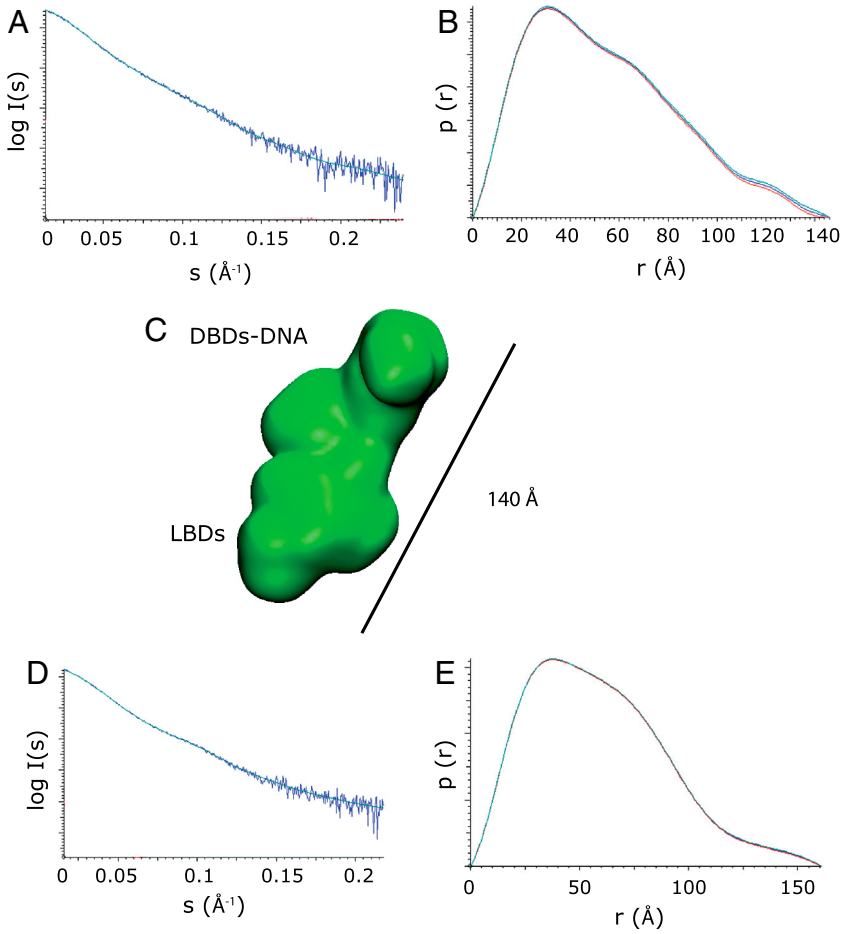

Fig. S10. Small angle X-ray scattering data. (*A*) Experimental scattering curve of RARαΔABF-RARαΔABF-DR5. (*B*) Pair distance distribution function P(r). (*C*) Most typical ab initio envelope of RARαΔABF-RARαΔABF-DR5 generated by DAMMIN (beads model) shows two domains separated by a region larger than in the envelope of RXRαΔAB-RARαΔABF-DR5. Experimental scattering curve of RARαΔAB-RARαΔAB-DR5-SRC-2 RID. (*D*) Corresponding pair distance distribution function P(r).

Table S1. Crystallographic data and refinement statistics of crystal structures of 9cis-RA-RARb LBD-SRC-1 NR2, TTNPB-RARb LBD-SRC-1 NR2, RU100132-ERa LBD-SRC-1 NR2 complexes

	RARβ LBD		ERα LBD
	9-cis RA complex (4DM8)	TTNPB complex (4DM6)	RU100132 (4DMA)
Data processing			
Space group	$P2_12_12_1$	$P2_12_12_1$	$P2_1$
Cell Dimensions (Å;°)	$a = 58.48$, $b = 83.62$, $c = 108.78$	$a = 58.09$, $b = 84.06$, $c = 102.14$	$a = 56.282$, $b = 81.788$, $c = 58.303$; $\beta = 111.17$
Resolution (Å)	20–2.3	20–1.9	30–2.3
Completeness (last shell)	95.6% (97.6%)	98.4% (100%)	96.6% (99.1%)
Rsym (last shell)	0.08 (0.28)	0.07 (0.40)	0.07 (0.12)
$\langle I/\sigma(I)\rangle$ (last shell)	13.6 (7.4)	27.2 (5.3)	12.8 (7.9)
Redundancy	4.1	5.0	3.1
Refinement statistics			
Rwork (no. of reflections)	22.4% (21,814)	20.6% (38,045)	20.5% (18,877)
Rfree (no. of reflections)	27.7% (1,094)	23.9% (2,003)	25.1% (2,067)
No. of protein atoms	3,969	3,922	3,977
No. of ligand atoms	52	44	42
No. of solvent molecules	128	178	120
rmsd bond length (Å)	0.006	0.01	0.007
rmsd bond angle (°)	1.07	1.08	1.15
$\langle B\rangle$			
Protein M1(M2)	52.8 (45.2)	36.1 (29.9)	31.9 (30.1)
Ligand M1(M2)	52.4 (50.0)	37.7 (30.7)	50.4 (50.7)
CoA M1(M2)	64.3 (55.9)	46.1 (33.7)	42.5 (36.5)

Same buffer as described in *Methods*.

Table S2. Elution volumes (mL) on S75 10/30 gel filtration column

Complexes	Elution volume (mL)			
	Complex	CoA	Dimer	Monomer
RARβ LBD apo				11.4
RARβ LBD-TTNPB				11.5
RARβ LBD-TTNPB-SRC-1 NR2			10.3	11.4
SRC-1 RID		9.6		
SRC-2 RID		9.8		
RARβ LBD-TTNPB-SRC-1 RID	8.8			
RARβ LBD-TTNPB+3eq SRC-2 RID	8.7	9.9		
RARα LBD apo				10 ;9
RARα LBD-*9 cis* RA				11.0
RARα LBD -TTNPB-SRC-1 NR2			10.0	10.9
RARα LBD-TTNPB-SRC-1 RID	8.7			10.8
RARγ LBD apo				11.0
RARγ LBD -*at* RA-SRC-1 NR2			10.3	11.3
RARγ LBD -*at*RA-SRC-1 RID	8.9			11.1

Table S3. Binding parameters derived from ITC measurements for SRC-1 NR2 (676-CPSSHSSLTERHKILHRLLQEGSPS-700) peptide or SRC-2 RID to NR LBD

		N	Kd (μM)	ΔH (cal/mol)	ΔS (cal/mol/K)
RARα LBD	SRC-1 NR2	1.87 ± 0.01	1.5 ± 0.1	−3,150 ± 20	16.1
	SRC-2 RID	0.83 ± 0.02	2.5 ± 0.2	−14,900 ± 400	−23.6
RARα E393Q LBD	SRC-1 NR2	2.3 ± 0.04	7 ± 0.1 (Kd1 = 3; Kd2 = 16)	−6,240 ± 170	3.0
	SRC-2 RID	0.78 ± 0.02	2.5 ± 0.2	−28,000 ± 500	−61
RXRα-RARα LBD	SRC-2 RID	0.81 ± 0.01	0.23 ± 0.005	−10,600 ± 110	−22.7
ERα LBD	SRC-2 RID	0.95 ± 0.01	0.65 ± 0.005	−22,500 ± 440	−45.9
ERα C530S LBD	SRC-2 RID	0.9 ± 0.01	0.26 ± 0.005	−35,500 ± 900	−87
ERα C530S E523Q LBD	SRC-2 RID	0.88 ± 0.02	0.35 ± 0.01	−53,100 ± 1,700	−146

The values for the affinity (K_d, dissociation constant) and enthalpy change (ΔH) accompanying the binding of SRC RID or NR2 peptide to NR LBD were obtained from the fit of a one-site model or two-site model, based on the binding of a ligand to a macromolecule using the law of mass action, to the corresponding ITC isotherms. N corresponds to the stoechiometry of the binding. Entropic contribution ($T\Delta S$) to binding was calculated from the relationship $T\Delta S = \Delta H - \Delta G$ with $\Delta G = \mathrm{RT}\ln K_d$, where R is the universal molar gas constant (1.99 cal/mol/K) and T is the absolute temperature (K). Errors were calculated from at least three independent measurements. All errors are given to one standard deviation.

Table S4. Small angle X-ray scattering parameters

Complexes	Rg, Å	D_{max}, Å
RARΔAB/RXRΔAB/DR5	44 ± 0.5	150 ± 10
RARΔAB/RARΔAB/DR5	43 ± 0.5	150 ± 10
RARΔAB/RARΔAB/DR5/SRC-2-2 RID	46 ± 0.5	165 ± 10
RARΔAB/RXRΔABm/DR5/SRC-2-2 RID	50 ± 0.5	170 ± 10

R_g and D_{max} are the radius of gyration and maximum size, respectively, calculated from the SAXS data. The forward scattering I(0) and the radii of gyration R_g were evaluated using the Guinier approximation (1), assuming that at very small angles ($s < 1.3/R_g$) the intensity is represented as $I(s) = I(0)\exp\{-(sR_g)2/3\}$. R_g and D_{max} were also computed from the entire scattering pattern using the indirect-transform package GNOM (2). Low resolution models were constructed ab initio using DAMMIN (3).

1. Guinier A (1939) Diffraction of X-rays of very small angles: Application to the study of ultramicroscopic phenomena. *Ann Phys* 12:161–237
2. Svergun DI (1992) Determination of the regularization parameter in indirect-transform methods using perceptual criteria. *J Appl Cryst* 25:495–503.
3. Svergun DI (1999) Restoring low resolution structure of biological macromolecules from solution scattering using simulated annealing. *Biophys J* 76:2879–2886.